Title: High-Throughput Optimization of Photochemical Reactions using Segmented-Flow Nanoelectrospray-Ionization Mass Spectrometry

Authors: Alexandra C. Sun; Daniel J. Steyer; Richard I. Robinson; Carol Ginsburg-Moraff; Scott Plummer; Jinhai Gao; Joseph W. Tucker; Dirk Alpers; Robert T. Kennedy; Corey R. J. Stephenson

To be cited as: 10.1002/ange.202301664

Link to VoR: https://doi.org/10.1002/ange.202301664

RESEARCH ARTICLE

High-Throughput Optimization of Photochemical Reactions using Segmented-Flow Nanoelectrospray-Ionization Mass Spectrometry

Alexandra C. Sun,[1†] Daniel J. Steyer, [1†] Richard I. Robinson,[2] Carol Ginsburg-Moraff,[2] Scott Plummer,[2] Jinhai Gao,[2] Joseph W. Tucker,[3] Dirk Alpers,[1] Corey R. J. Stephenson,[1*] Robert T. Kennedy[1*]

[a] Dr. A. C. Sun, Dr. D. J. Steyer, Dr. D. Alpers, Prof. C. R. J. Stephenson, Prof. R. T. Kennedy
Department of Chemistry
University of Michigan
Ann Arbor, MI 48109 USA
E-mail: crjsteph@umich.edu, rtkenn@umich.edu
[b] Dr. R. I. Robinson, C. Ginsburg-Moraff, Dr. S. Plummer, Dr. J. Gao
Global Discovery Chemistry
Novartis Institutes for Biomedical Research
Cambridge, MA 02139 USA
[c] Dr. J. W. Tucker
Medicine Design
Pfizer Inc.
Groton, CT 06340 USA
[d] †These authors contributed equally to this work.

Supporting information for this article is given via a link at the end of the document.

Abstract: Within the realm of drug discovery, high-throughput experimentation techniques enable the rapid optimization of reactions and expedited generation of drug compound libraries for biological and pharmacokinetic evaluation. Herein we report the development of a segmented flow mass spectrometry-based platform to enable the rapid exploration of photoredox reactions for early-stage drug discovery. Specifically, microwell plate-based photochemical reaction screens were reformatted to segmented flow format to enable delivery to nanoelectrospray ionization-mass spectrometry analysis. This approach was demonstrated for the late-stage modification of complex drug scaffolds, as well as the subsequent structure-activity relationship evaluation of synthesized analogs. This technology is anticipated to expand the robust capabilities of photoredox catalysis in drug discovery by enabling high-throughput library diversification.

Introduction

In the search for breakthrough medicines, materials, and agrichemicals, the accelerated preparation of complex small molecules in a miniaturized fashion can have a profound impact on reducing chemical footprint while expanding upon reaction space.[1-8] High-throughput experimentation (HTE) technologies offer avenues for rapid data collection and process automation, and their implementation in organic synthesis have enabled the expedited discovery and optimization of various reaction manifolds.[9-18] From a pharmaceutical standpoint, the rapid development and application of novel synthetic methodology play a central role in accelerating access to highly functionalized drug leads. Given the short supply of substrate material at the start of a drug discovery program, it is often necessary to decrease the scale of experimentation to access broader chemical space.[17,18-25] The use of HTE techniques can streamline approaches for the exploration of myriad catalysts and reaction conditions in a time and resource-efficient manner. Recent advances in miniaturized HTE have supported the diversification of expansive pharmaceutical libraries *via* palladium-catalyzed C–C, C–O, and C–N bond forming reactions at nanomole scale, using both continuous flow and plate-based approaches.[17,18-27] Furthermore, platforms that integrate high-throughput reaction optimization with subsequent biological evaluation provide additional opportunities for streamlining bioactive molecular discovery.[18]

Critical to the application of HTE workflows is the integration of high-throughput analytical instrumentation to provide rapid analysis of reaction mixtures. Mass spectrometry (MS) is an appealing tool for application in HTE, due to the high degree of chemical information and specificity imparted in its measurements.[17,19] Application of rapid liquid chromatography (LC) has enabled MS-based analysis of reactions at a throughput of up to 0.05 samples/s.[17,19] A major limitation in these systems is the use of a time-consuming LC separation before detection. As such, expediting sample introduction to MS analysis represents a natural next step for improving such screening approaches.[28-37]

A proven approach for rapid sample introduction to electrospray ionization-MS (ESI-MS) is the use of droplet microfluidics. With the use of an immiscible carrier phase, segmented droplet samples can be flowed sequentially to a mass spectrometer for rapid analysis. This approach has seen application across areas such as enzyme evolution, drug discovery, and organic synthesis. Electrospray of droplet samples is achieved either by directly performing ESI on individual droplets or by introduction of droplets to a continuously spraying sheath liquid. Droplet-based ESI-MS screening of enzymatic reactions contained in well plates has been achieved at throughputs of up to 4.5 droplets/s.[38-40] Systems pairing ESI emitters directly to microfluidic devices have shown capability of even higher throughputs, with one example achieving analysis at up to 33 droplets/s.[41] The use of low flow nanoESI-MS (nESI-MS) has also been applied in the analysis of droplet samples.[40-43] Benefits of employing nESI in place of standard ESI include heightened ionization efficiency in the presence of sample matrices that suppress analyte ionization, as well as the use of gentler conditions to enable the observation of more labile molecular ions. Both benefits complement a MS-based HTE platform, as they increase the likelihood of observing molecular ions across a range of different sample compositions and molecular analytes.

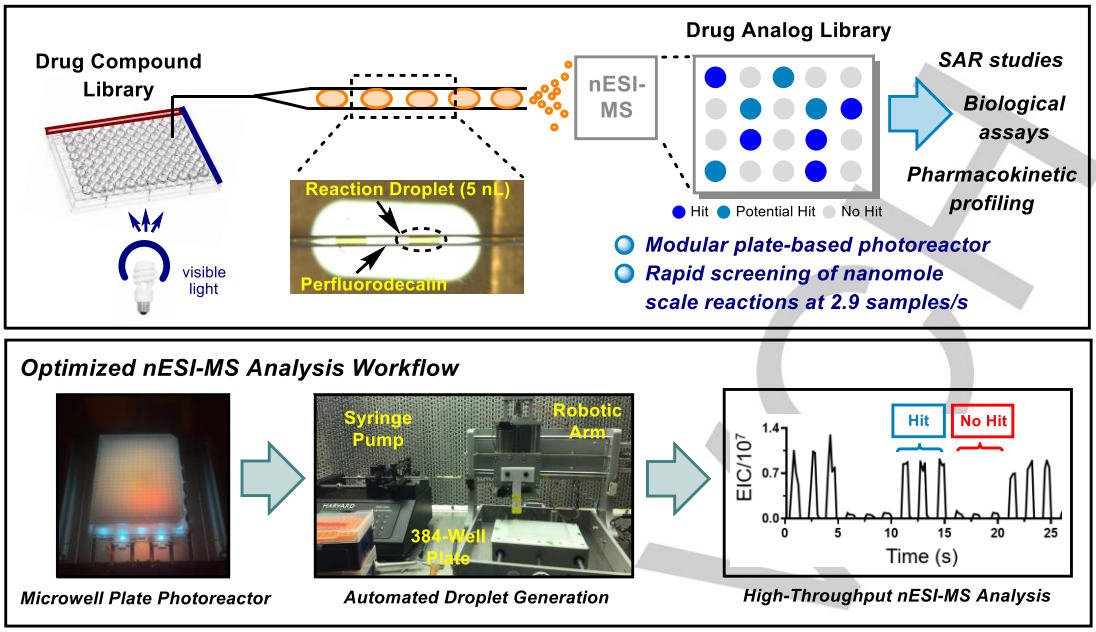

Figure 1. Highlights of droplet-based nESI-MS screening platform. (A) Overview of droplet nESI-MS platform for screening plate-based photochemical reactions. (B) Development of a microwell plate photoreactor and integration into a nESI-MS analysis workflow.

As it stands, analytical platforms that combine droplet microfluidics and MS for organic synthesis applications have been significantly limited in scope.[44-46] The development of novel droplet microfluidic-MS approaches and application to chemical transformations of rising interest could significantly drive further innovations in HTE. Over the past decade, photoredox catalysis has risen to the forefront of organic synthesis by enabling rapid access to nontraditional bond constructions and aiding in sustainability efforts through the use of visible light.[47-49] In particular, photoredox catalysis has gained meaningful traction in medicinal chemistry applications by providing versatile access to scaffolds and building blocks that previously required a significant number of operations.[50-51] Nonetheless, one key challenge to achieving widespread implementation of photoredox catalysis within medicinal chemistry stems from the scalability and generality of existing reactor platforms. To use these visible light-driven methods to their full potential, development of a user-friendly benchtop photoreactor featuring reaction screening and facile scale-up capabilities is needed. In our previous report, we have demonstrated the utility of droplet ESI-MS in enabling picomole-scale photochemical reaction discovery in flow by performing in-droplet reactions and analyzing at throughputs of up to 0.3 samples/s.[46] This work focuses on the development of a complementary platform to screen photoredox catalysis reactions in a plate-based format. By transferring these samples to segmented droplet flow, nESI-MS analysis (up to 2.9 droplet/s) could be performed for the rapid characterization of late-stage functionalization libraries to enable subsequent scale-up and biological evaluation (**Figure 1**).

Results and Discussion

Development of a plate-based photoreactor and preliminary nESI-MS studies

Our studies into leveraging droplet microfluidics technology for reaction discovery have been centered on the development of a nESI-MS platform for the high-throughput analysis of photochemical late-stage functionalization reactions. We chose to employ a radical perfluoroalkylation strategy developed by the Stephenson group[52-55] as a model system for the diversification of pharmaceutical compound libraries. Namely, we have developed a platform that interfaces a custom plate-based photoreactor with nESI-MS analysis with to accommodate the rapid screening of complex drug molecule libraries in nanoliter volume droplets. We envisioned that this setup would be amenable to applications including the late-stage functionalization of drug scaffolds and rapid optimization of substrate-specific reaction conditions.

We began our studies by identifying a photoreactor that could accommodate well plate-based reaction screens. While several commercially available photoreactors have been designed for parallel synthesis applications (see SI), there are significant limitations associated with these systems, including incompatibility with standard well plate dimensions as well as the use of low intensity light-emitting diodes (LEDs). With the objective of maximizing photon flux while enhancing reproducibility, we designed a modular benchtop photoreactor for irradiation of microwell plate reactions using high-powered Cree Royal Blue XTE LEDs (2 W per LED). We constructed a 25 LED array (approx. 50 W total output) photoreactor to accommodate the dimensions of a standard 96, 384, or 1536 well plate. Our workflow (**Figure 1B**) for droplet generation involves loading a pre-mixed reaction solution onto a microwell plate, followed by blue light irradiation. A small fraction of each reaction was then withdrawn and diluted. The dilution served to both quench the reaction and facilitate MS analysis, as analytes of high concentration (> 1 mM) can lead to saturation of MS signal and contamination of the MS source. 8 μL of each diluted reaction mixture was deposited into a separate well plate and covered with perfluorodecalin (PFD) for subsequent droplet formation in perfluoroalkoxy (PFA) tubing (150 x 360 μm internal diameter x outer diameter). Droplet samples (5-10 nL) were generated from microwell plates using equipment and methods previously reported.[38,39,56]

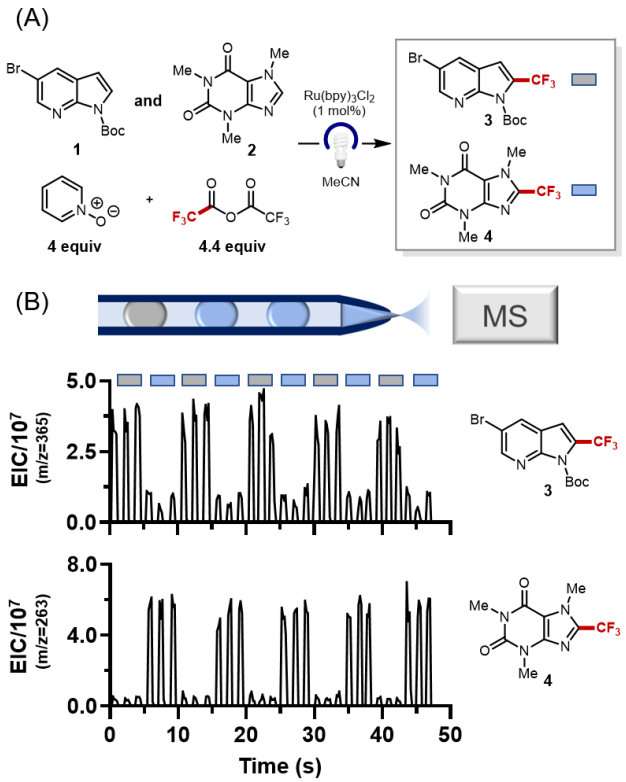

Figure 2. Droplet nESI-MS analysis of photoredox trifluoromethylation reactions. (A) Photoredox trifluoromethylation of caffeine and 5-Br-7-(*N*-Boc)azaindole substrates. (B) Droplet nESI-MS analysis of caffeine and 5-Br-7-(*N*-Boc)azaindole trifluoromethylation reactions. Droplet trains of repeating 3x3 format were analyzed by nESI-MS at 0.67 droplets/s. The two traces represent the extracted m/z for **3** (m/z=367, top) and **4** (m/z=263, bottom). Bars above traces represent droplets formed from reactions of substrates **1** (grey) and **2** (blue).

To demonstrate the general capabilities of our system, we examined the photoredox trifluoromethylation of *N*-Boc-5-bromo-7-azaindole and caffeine substrates (**Figure 2**).[52] Sample droplets (8 nL) were formed in a repeating 3x3 fashion. Droplet analysis was performed at a rate of 0.67 droplets/s by infusing the droplet train at 322 nL/min into the nESI source, allowing for triplicate sample analysis to be performed in under 5 s. Analysis throughput at this stage was limited by the scanning rate of our mass spectrometer, which required 170 ms per scan. By extracting out the m/z values associated with our expected products (m/z 263 for trifluoromethyl caffeine, m/z 365 for trifluoromethyl *N*-Boc-5-bromo-7-azaindole), we were able to successfully monitor product formation in both reactions. As shown in **Figure 3**, two separate droplet populations can be observed in the anticipated 3x3 fashion. Droplets that show high response for product formation in one trace show low response in the other, yielding an offset product signal pattern across the two traces. These results not only validate the capability of our system to detect product formation, but also demonstrate the ability to perform rapid analysis while maintaining the identity of the individual samples. Also of note is the effect of nESI for product detection. Applying low flow rates reduces the required temperatures and electric potentials to perform electrospray and desolvate analytes. These gentler conditions can lead to observation of labile molecular ions that may be lost during standard ESI, as we observed with trifluoromethyl *N*-Boc-5-bromo-7-azaindole (see SI).

nESI-MS analysis of late-stage functionalization libraries

With the developed system, we aimed to achieve three goals: (1) accomplish late-stage functionalization using diverse radical coupling partners, (2) perform high-throughput optimization of reaction conditions for individual drug scaffolds, and (3) demonstrate the immediate benefit of using droplet microfluidic nESI-MS for the late-stage diversification of drug compound libraries and its integration into structure-activity relationship (SAR) studies and biological assays in a medicinal chemistry setting. To achieve our first objective of performing the late-stage functionalization of complex drug molecules, we carried out the fluoroalkylation (CF_3, CF_2H, CF_2Cl) of 17 drug and drug-like compounds provided by a commercial library from Pfizer (**Figure 3**).[58] Reactions were irradiated with blue light for 1 h in a 384 polypropylene well plate prior to dilution and subsequent droplet generation for nESI-MS analysis. To enhance substrate solubility and maintain homogeneity of reactions, substrate stock solutions were prepared using a 10% DMF/MeCN solvent system. Excess trifluoroacetic anhydride (16 equiv) was added to accommodate acylation by nucleophilic functionalities (e.g. free amines and alcohols) on substrates within our targeted library.

Upon generating reaction droplets in triplicate, nESI-MS analysis was performed at a throughput of 0.67 droplets/s. Control samples containing no added substrate were run to differentiate between MS signals that derived from the reaction of interest and signals that were simply artifacts of our sample matrices. Shown in **Figure 3A** is the extracted ion trace (523 m/z) for the trifluoromethylated product of PF1, Verapamil HCl. Upon analysis of the droplets containing compound 1, a significant increase in signal intensity is observed in comparison to the control samples, suggesting successful product formation. This same approach was applied to each of the tested substrates in our library. We were able to identify several "hit" reactions for each perfluoroalkylation reaction, in which desired product m/z signals were significantly elevated relative to control signals. With the aim of qualitatively assigning "hit"/"no hit" responses to each reaction, we conducted analyses to assess the statistical relevance of our product m/z signals over background noise. A two-sample t-test was performed, in which each reaction of interest was compared against the control samples to confirm the presence of newly generated product m/z signals. Reactions were deemed a hit if they achieved a $P<0.01$. Across 5 distinct substrates that yielded "hit" responses, significant product m/z signal increases were observed for all three fluoroalkylation conditions, demonstrating the capability of our method to successfully detect product formation across a diversity of complex small molecules (**Figure 3B**). MS counts were also utilized to show the strength of "hit" responses. A $\log_{10}$(product response-control response) test was used to gauge the magnitude of signal increase and in turn, highlight promising reaction conditions.

Three "hit" reactions were scaled up to 0.1 mmol scale for subsequent purification and product isolation to further validate our nESI-MS results. Successful isolation of bis-trifluoromethylated (45% yield) varenicline tartrate was achieved, validating our corresponding nESI-MS screen data. Isolation of trifluoromethylated Verapamil HCl and PF15 products was

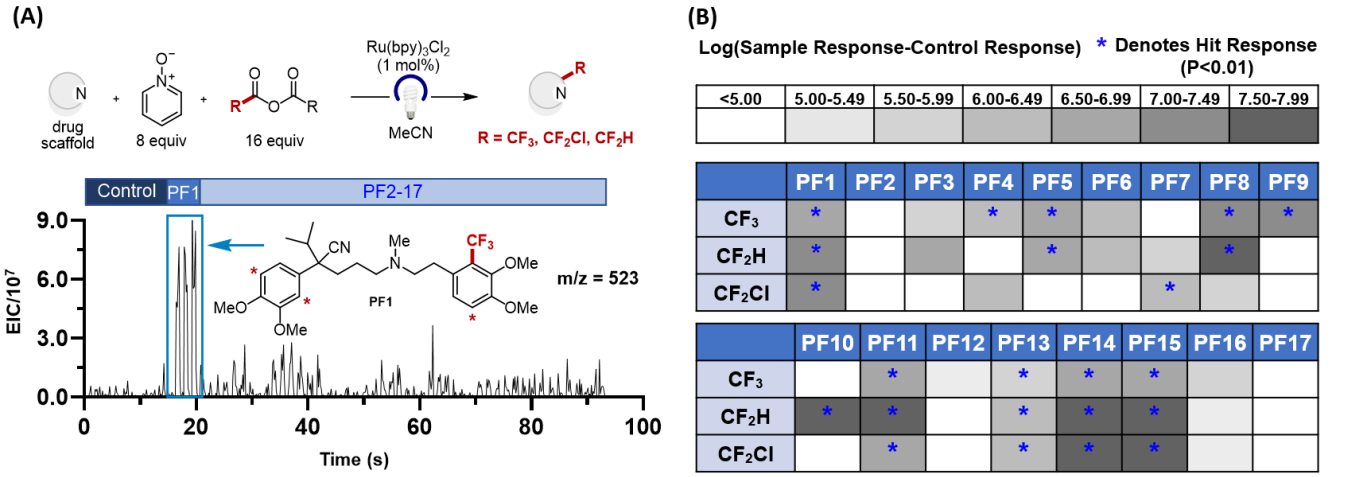

Figure 3. Screen for late-stage fluoroalkylation of pharmaceutical compounds by droplet nESI-MS. (A) General scheme for fluoroalkylation of 17-compound library (top) and mass trace for predicted PF1 product (bottom). Displayed is the m/z = 523, which is the predicted MH^+ ion of mono-trifluoromethylated verapamil HCl. Asterisks denote additional formation of regioisomers. (B) Coloration on heat map describes increased response for desired product MH^+ ion over control, while blue asterisks denote statistical significance in response increase.

attempted to elucidate regioisomer formation; however, desired products could not be successfully isolated due to low yields and product decomposition upon column chromatography. The HTE data obtained from our screen provided insight into several reactivity trends that arose from varying substrates and perfluoroalkyl radical reagents. Our screen revealed "hit" responses across 11 substrates (65% of 17 compound library), as well as successful product formation across all three perfluoroalkylation conditions for 5 substrates (compounds PF 1, 11, 13, 14, and 15). Among our "hit" compounds, a variety of heteroarene scaffolds were accessible, including quinoxalines, furo[2,3]pyridines, quinazolinones, pyrrolopyrimidines, and pyrrolopyridinones. We were gratified to see that several of these "hit" response scaffolds expanded upon the scope of structures formerly reported by the Stephenson group.[17a,c] These results highlight the successful application of this methodology for substrates of increased complexity and diverse functionality. Among substrates that did not yield any product formation (PF 2, 3, 6, 12, 16, 17), we noted that the presence of electron rich alkyl amine motifs (PF 2, 12, 16) could be problematic, as these functionalities can be prone to single electron oxidation and subsequent decomposition. Additionally, the presence of sterically hindered aromatic groups (PF 12) could further hinder radical functionalization.

High-throughput optimization of photoredox reactions

In addition to enabling the accelerated late-stage functionalization of diverse pharmaceuticals, our platform can also be utilized for the high-throughput optimization of photoredox reaction conditions. With the broader aim of obtaining quantitative insight into product conversion and reaction kinetics, as well as expanding upon screen parameters to include various solvent systems, we have developed nESI-MS methods for measuring product formation. To expand upon our platform's high-throughput reaction optimization capabilities, we examined a broad set of parameters for the radical trifluoromethylation of caffeine, including solvents, photocatalysts, and heterocyclic *N*-oxide reagents (**Figure 4**). Specifically, we set out to establish a robust analytical method to quantitate product conversion. To lower background signals, MS-MS analysis was performed to target a specific fragmentation pattern arising from the trifluoromethylated caffeine analyte (m/z = 263→206).[59] We also needed to address challenges associated with ion suppression, as changes in the sample matrix (e.g. solvent environment) can drastically affect analyte ionization and observed MS response. While this effect is typically resolved through sample cleanup methods (e.g. liquid chromatography and chemical extractions), we pursued a methodology allowing direct analysis of droplet samples to maximize throughput.

By using the radical trifluoromethylation of caffeine as our model reaction system, we have demonstrated successful screening of co-solvent systems including 10% co-solvent/MeCN (co-solvents: DMF, DMA, CH_2Cl_2, $MeNO_2$, DMSO). In the presence of these co-solvents, analyte response saw as much as a 4-fold drop, despite constant analyte concentrations (SI). Without correction, this effect would confound direct comparison between conditions. To overcome matrix effects, we explored three methods: the use of standard addition, internal standard, and higher dilution factor. Each of these methods demonstrated capability in both normalizing matrix effects and observing changes in analyte concentration. A breakdown of the results and relative merits of each method can be found in the SI. Moving forward, we chose to use ethyltheophylline as an internal standard,[60] as it provided excellent results with regards to signal normalization and minimizing variability in measurement. A 72-reaction screen was then performed to optimize the caffeine trifluoromethylation reaction by screening parameters including photocatalyst, *N*-oxide reagent, and co-solvent (**Figure 4A**). The triplicate analysis of all 72 reactions was performed in 380 s (0.67 droplets/s). Successful product formation was observed over a wide range of conditions (**Figure 4B**).

Solvent choice was found to have the largest influence on product formation. The use of 10% DMSO (6) yielded poor turnover, while 10% DMF and DMA (4 and 5 respectively) gave the highest turnover across multiple conditions. These results highlight the importance of addressing matrix effects. DMF and DMA were both observed to greatly suppress product signal, and as such, would not likely have been viable co-solvents prior to adjusting for variable ionization efficiencies. Five of our top performing reactions were selected for subsequent scale-up on

300 µmol scale and irradiated in a 96 well plate (**Figure 4C**). Gratifyingly, nESI-MS results suggested that the yields obtained

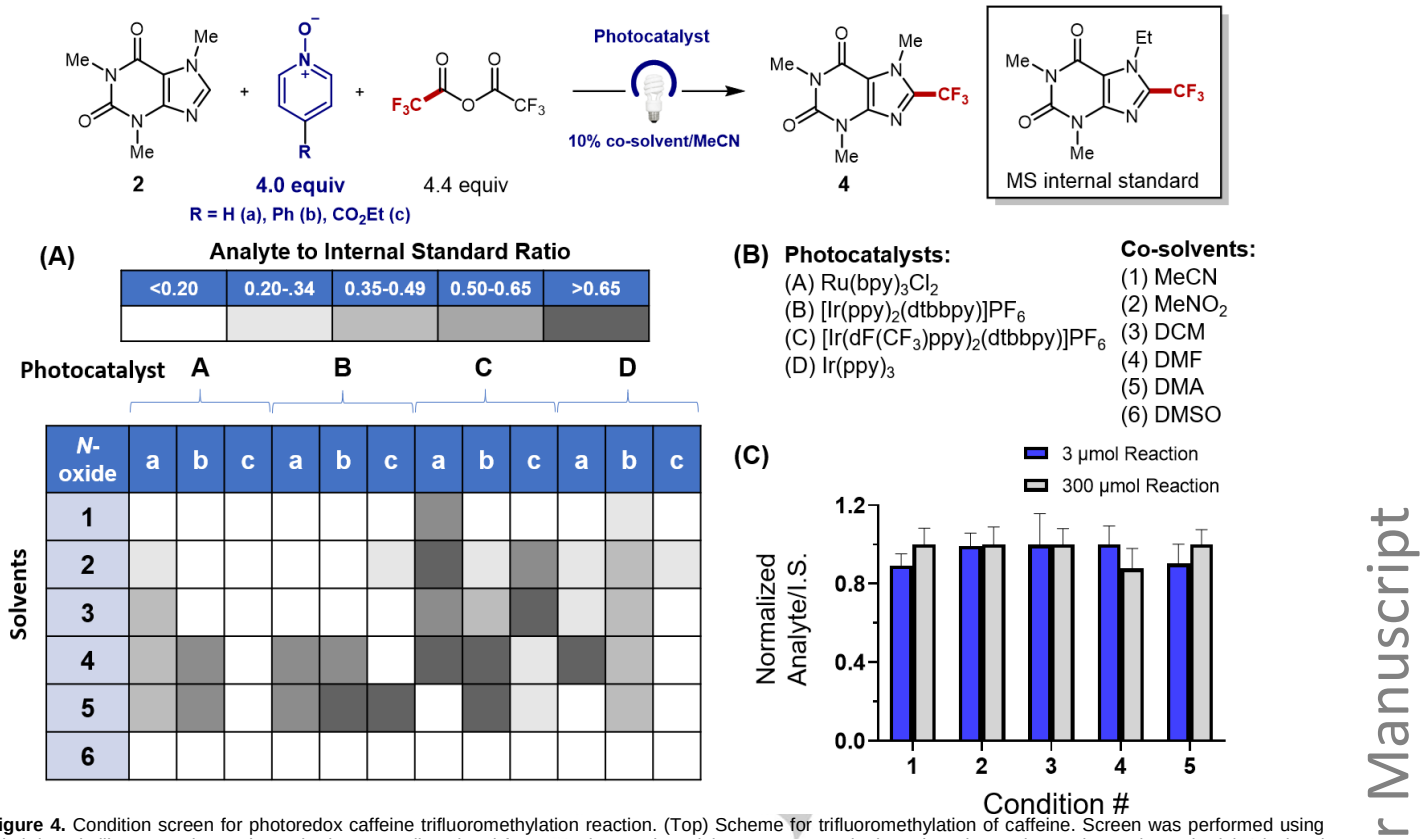

Figure 4. Condition screen for photoredox caffeine trifluoromethylation reaction. (Top) Scheme for trifluoromethylation of caffeine. Screen was performed using ethyl theophylline as an internal standard to normalize signal from reaction product. (A) Heat map results based on the analyte to internal standard (I.S.) signal ratios. Each cell represents the average of 3 droplets. Darker shading represents a higher observed ratio, indicating increased product formation. (B) Photocatalysts and co-solvents evaluated across 72 reaction screen. (C) Demonstration of reliability in scaling up reactions. Droplet nESI-MS comparison (n=10 droplets) of samples run at screen scale (3 µmol) and 100x scale (300 µmol) showed similar response for all 5 different reaction conditions. Normalization of results was performed within each pairing. The top 5 reaction conditions are listed in order as conditions 1-5.

from the scale-up reaction show strong correlation with that of our small-scale screens, which further validates the scalability of our screening method and the opportunity to quantitatively benchmark reaction performance in a high-throughput manner.

Late-stage functionalization and biological evaluation of compounds

With the goal of applying our HTE platform towards a medicinal chemistry setting, we have employed our nESI-MS system in screening a diverse library of pharmaceutical intermediates, provided by Novartis, for late-stage modification. Specifically, we set out to screen a library of 15 compounds, which have previously been investigated as firefly luciferase (FLuc) inhibitors, for late-stage C–H alkylation (CF_3, CH_3, cyclopropyl).[60] By providing high-throughput access to photochemical C–H alkylation, we aimed to facilitate the diversification of structural libraries and enable the rapid generation of drug analogs for subsequent biological evaluation. In our initial library screen, we irradiated a 15 x 3 array of reactions to screen 15 Novartis drug scaffolds using 3 radical precursors with our microwell plate photoreactor. Following dilution and droplet generation of each reaction sample in triplicate, we performed nESI-MS analysis to identify hit responses using statistical analysis. We were able to observe hit responses (Figure 5A) from 2 parent compounds (NV1 and NV4) and their corresponding daughter fragments (NV8 and NV9). Our MS results suggested that in the absence of an activating ester moiety, daughter fragments NV10 and NV11 did not undergo successful C–H alkylation. Additionally, functionalization products were observed for daughter fragments NV13 and NV15, while their respective parent compounds did not give rise to alkylated analogs (see SI for details). To validate our nESI-MS screen results, 6 of our top-performing substrates (NV1, NV3, NV4, NV8, NV9, NV15) were selected for scale-up and subjected to the same 3 photochemical alkylation conditions at 0.1 mmol scale (Figure 6A). To generate microgram amounts of material for subsequent biological assays, mass-directed purification techniques were used to perform product isolation. Notably, we were able to successfully isolate 11 products (Figure 5B), all of which had been labeled as "hits" in our initial nanomole scale screen. Acylation of the nucleophilic amine group was observed in the trifluoromethylation product of NV9, which could explain its absence as a hit in our follow-up screen. While product masses were detected upon UPLC-MS analysis of methylated NV4, isolation was unsuccessful, most likely due to low levels of product formation. NMR characterization of NV1- CH_3 and NV1-C_3H_5 suggested the formation of off-target products *via* de-ethylation and acylation of the diethylamine group. Loss of the ethyl group was confirmed by predictive NMR studies. Interestingly, these products were originally designated as hits by nESI-MS analysis, as they have the same masses as the desired C-H functionalized products. Subsequent isolation and characterization revealed them to be separate isomers. Control experiments suggest that loss of the ethyl group occurs under

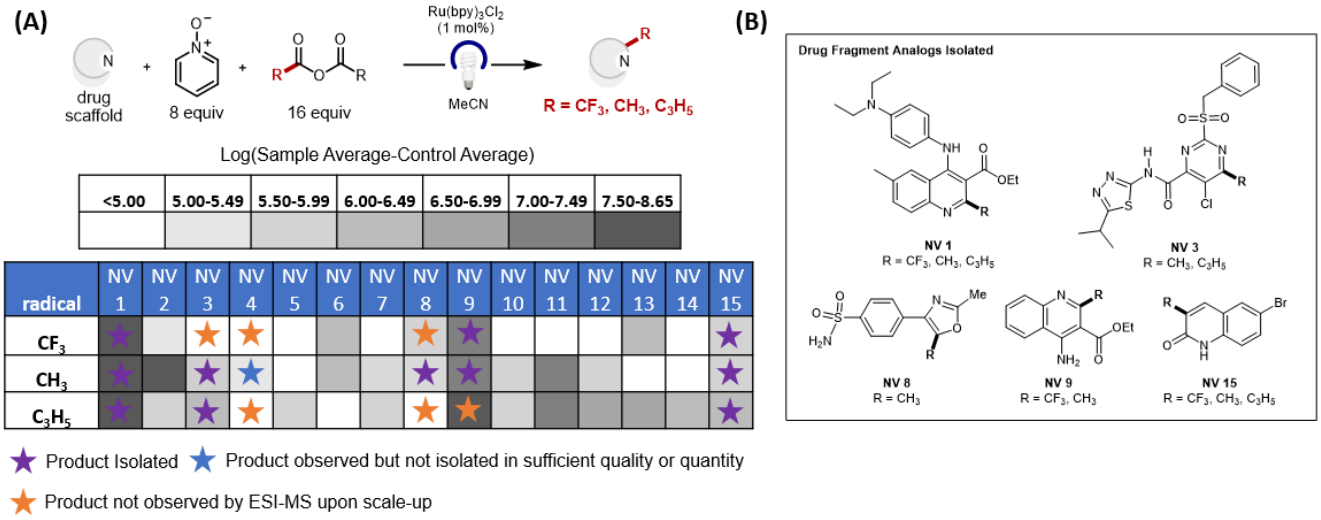

Figure 5. Late-stage functionalization of Novartis drug fragment library. (A) Droplet nESI-MS screen of perfluoroalkylation conditions on 1 µmol scale. Coloration on heat map describes increased response for desired product MH^+ ion over that of the control. The star symbols denote the outcome of product isolation upon 0.1 mmol scale-up. (B) Drug fragment analogs isolated in 0.1 mmol scale-up.

photochemical conditions, likely driven by single-electron oxidation of the amine. Five of our synthesized analogues (NV1-subsequent biological assays upon NMR analysis. These five compounds, along with our original 15 library members (NV1-NV15), were run through an RLuc (renilla luciferase) assay[61] to measure inhibition of the renilla luciferase enzyme (**Figure 6**; see

CH_3, NV1-C_3H_5, NV9-CF_3, NV3-C_3H_5, NV15-CF_3) were isolated in sufficient quantity and determined to meet purity criteria for

SI for details of full screen). Assay results suggest that while parent scaffolds NV1 and NV showed RLuc activity, their synthesized analogues (NV1-CH_3, NV1-C_3H_5, NV15-CF_3) did not show any significant activity.

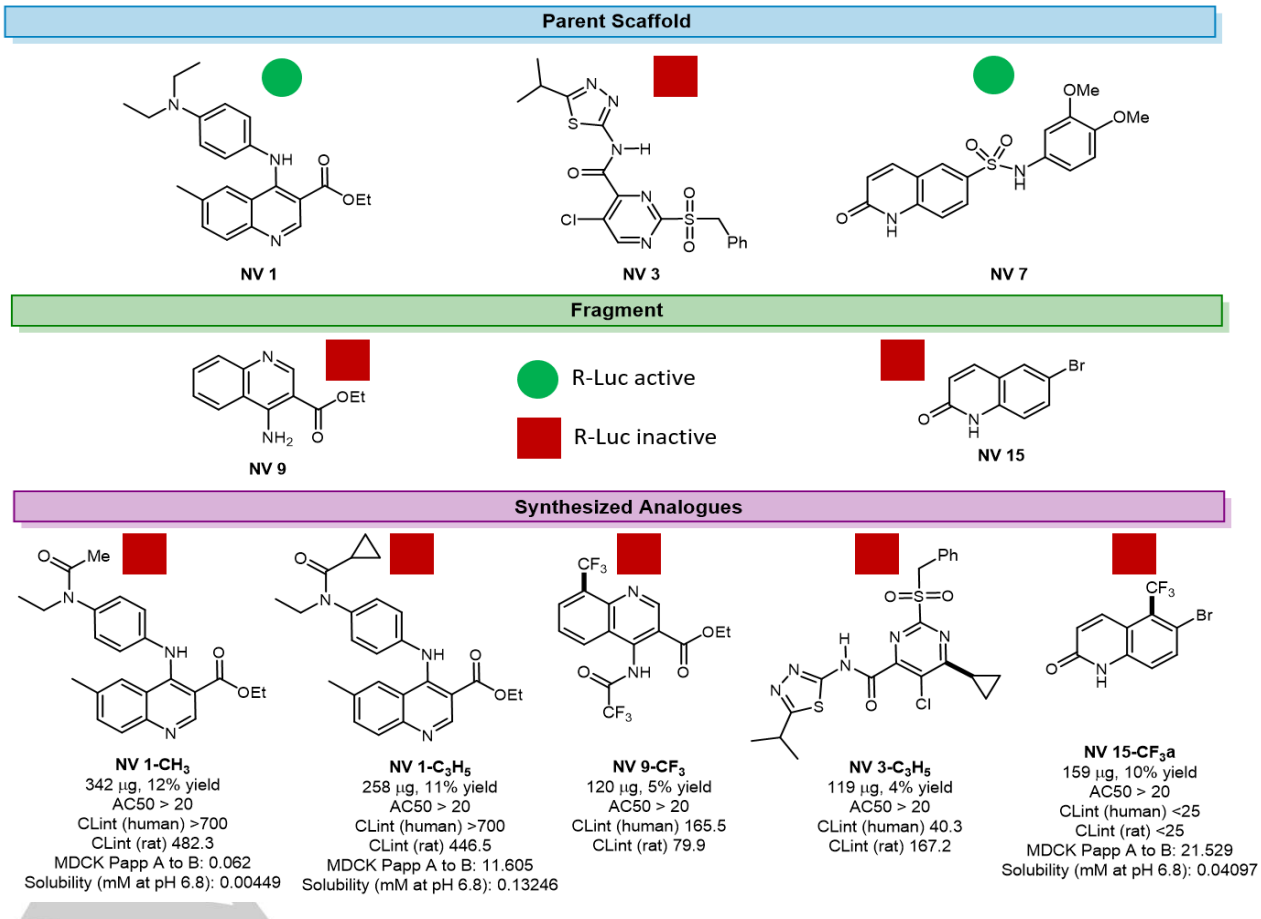

Figure 6. RLuc assay activity of select library compounds and microscale profiling assays. Green circles denote inactivity in R-Luc assay, while red squares denote RLuc assay activity. AC50 represents the concentration (µM) of a compound at which 50% of the renilla luciferase enzyme is inhibited. The CLint values measure the half-life of the compound divided by protein concentration in the assay. Papp (P apparent) measures the ratio of the compound in the apical layer to compound in the basal layer of MDCK (canine epithelial) cells. See supplementary information file for assay details.

Compounds NV9-CF_3 and NV3-C_3H_5 were observed to be RLuc inactive, as was reported for their parent scaffolds (NV3 and NV5). Additionally, the five synthesized analogues and NV1-NV15 were subjected to Novartis' standard microscale profiling assays for clearance, permeability, and solubility (Figure 6, see SI for details). While the examined hits from our screen did not exhibit biological activity, these studies effectively demonstrate how droplet nESI-MS can be used both to rapidly characterize complex pharmaceutical libraries, as well as to identify viable targets for SAR studies and biological profiling.

Increasing nESI-MS analytical throughput

Finally, we explored our platform's potential for operating at even higher throughputs. Throughout these studies, the throughput established in our initial demonstration (0.67 droplets/s) was used. Applying faster scanning instrumentation or a more focused m/z window would allow for higher throughputs to be achieved in future studies. In SI Figure S19, we showed that our nESI setup can process upwards of 2.9 droplets/s when monitoring a single m/z value. This throughput would allow for a 384 microwell plate to be analyzed in triplicate in under 7 min. For reference, the aforementioned work applying rapid LC-MS for screening synthetic reactions would require 422 minutes to achieve this same task.[17] With this degree of improvement, larger screens (>1000 reactions) could be accomplished in a matter of hours or even minutes.

Conclusion

In summary, an HTE platform for screening visible light-driven reactions was developed and successfully applied to photochemical reaction discovery and optimization. Simultaneous irradiation of samples in microwell plates, followed by translation into segmented droplets post-reaction facilitated rapid reaction screening and delivery to downstream analysis. The use of nESI-MS provided detection of a diverse population of reaction products with minimal assay development, as well as highly gentle ionization for the observation of labile species. The implementation of methods to address variable ionization efficiency in droplet nESI-MS analysis enabled the screening across a variety of photoredox reaction conditions. Screening of photoredox catalysis fluoroalkylation reactions was performed with the concerted objectives of enabling reaction discovery and high throughput optimization of 'hit' reaction conditions. nESI-MS analysis throughput as high as 2.9 samples/s was demonstrated, which would drastically push forward the limits in the high-throughput MS analysis of photoredox droplet reaction samples. Successful translation of nanomole-scale conditions to millimole-scale reactions was further demonstrated, highlighting the ability to concertedly perform rapid reaction discovery as well as subsequent scale-up for application in biological assays and profiling. The systems and methodologies presented show great promise for future work in visible light-driven reaction design and rapid diversification of pharmaceutical libraries to provide enhanced material and time efficiency in drug discovery.

Acknowledgements

The authors acknowledge the financial support for this research from the NSF (CBET-1604087, CHE-1900266, and CHE-2154668) and the University of Michigan. This manuscript was developed with the support of the American Chemical Society Green Chemistry Institute Pharmaceutical Roundtable (ACS GCIPR). The ACS GCI is a not-for-profit organization whose mission is to catalyze and enable the implementation of green and sustainable chemistry throughout the global chemistry enterprise. The ACS GCI Pharmaceutical Roundtable is composed of pharmaceutical and biotechnology companies and was established to encourage innovation while catalyzing the integration of green chemistry and green engineering in the pharmaceutical industry. The activities of the Roundtable reflect its members' shared belief that the pursuit of green chemistry and engineering is imperative for business and environmental sustainability. This material is based on work supported by an NSF Graduate Research Fellowship (Grant DGE 1256260) (A.C.S.).

Keywords: photocatalysis • microfluidics • high-throughput experimentation • mass spectrometry • continuous flow

References

[1] J. R. Schmink, A. Bellomo, S. Berritt, *Aldrichimica Acta* **2013**, *46*, 71.
[2] S. W. Krska, D. A. DiRocco, S. D. Dreher, M. Shevlin, *Acc. Chem. Res.* **2017**, *50*, 2976.
[3] S. Chow, S. Liver, A. Nelson, *Nat. Rev. Chem.* **2018**, *2*, 174.
[4] P. S. Gromski, A. B. Henson, J. M. Granda, L. Cronin, *Nat. Rev. Chem.* **2019**, *3*, 119.
[5] C. L. Allen, D. C. Leitch, M. S. Anson, M. A. Zajac, *Nat. Catal.* **2019**, *2*, 2.
[6] A. Milo, *Science* **2019**, *363*, 122.
[7] P. R. Fitzgerald, B. M. Paegel, *Chem. Rev.* **2021**, *121*, 7155.
[8] R. Grainger, T. D. Heightman, S. V. Ley, F. Lima, C. N. Johnson, *Chem. Sci.* **2019**, *10*, 2264.
[9] A. McNally, C. K. Prier, D. W. C. MacMillan, *Science* **2011**, *334*, 1114.
[10] D. W. Robbins, J. F. A. Hartwig, *Science* **2011**, *333*, 1423.
[11] A. Bellomo, N. Celebi-Olcum, X. Bu, N. Rivera, R. T. Ruck, *Angew. Chem. Int. Ed.* **2012**, *51*, 6912.
[12] M. R. Friedfeld, M. Shevlin, J. M. Hoyt, S. W. Krska, M. T. Tudge, P. J. Chirik, *Science* **2013**, *342*, 1076.
[13] D. A. DiRocco, K. Dykstra, S. Krska, P. Vachal, D. V. Conway, M. T. Tudge, *Angew. Chem. Int. Ed.* **2014**, *53*, 4802.
[14] K. D. Collins, T. Gensch, F. Glorius, *Nat. Chem.* **2014**, *6*, 859.
[15] S. Monfette, J. M. Blacquiere, D. E. Fogg, *Organometallics* **2011**, *30*, 36.
[16] S. M. Mennen, C. Alhambra, L. Allen, M. Barberis, S. Berritt, T. A. Brandt, A. D. Campbell, J. Castañón, A. H. Cherney, M. Christensen, D. B. Damon, J. Eugenio de Diego, S. García-Cerrada, P. García-Losada, R. Haro, J. Janey, D. C. Leitch, L. Li, F. Liu, P. C. Lobben, D. W. C. MacMillan, J. Magano, E. McInturff, S. Monfette, R. J. Post, D. Schultz, B. J. Sitter, J. M. Stevens, I. I. Strambeanu, J. Twilton, K. Wang, M. A. Zajac, *Org. Process Res. Dev.* **2019**, *23*, 1213.
[17] A. B. Santanilla, *Science* **2015**, *347*, 443.
[18] N. J. Gesmundo, B. Sauvagnat, P. J. Curran, M. P. Richards, C. L. Andrews, P. J. Dandliker, T. Cernak, *Nature* **2018**, *557*, 228.
[19] D. Perera, J. W. Tucker, S. Brahmbhatt, C. J. Helal, A. Chong, W. Farrell, P. Richardson, N. W. Sach, *Science* **2018**, *359*, 429.
[20] J. Welch, *React. Chem. Eng.* **2019**, *4*, 1985.
[21] T. W. Cooper, I. B. Campbell, S. J. Macdonald, *Angew. Chem., Int. Ed.* **2010**, *49*, 8082.
[22] S. D. Roughley, A. M. Jordan, *J. Med. Chem.* **2011**, *54*, 345.
[23] A. Nadin, C. Hattotuwagama, I. Churcher, *Angew. Chem., Int. Ed.* **2012**, *51*, 1114.
[24] P. M. Murray, S. N. G. Tyler, J. D. Moseley, *Org. Process Res. Dev.* **2013**, *17*, 40.
[25] T. Rodrigues, P. Schneider, G. Schenider, *Angew. Chem., Int. Ed.* **2014**, *53*, 5750.

[26] Y. J. Hwang, C. W. Coley, M., Abolhasani, A. L. Marzinzik, G. Koch, C. Spanka, H. Lehmann, K. F. Jensen, *Chem. Commun.* **2017**, *53*, 6649.
[27] A-C. Bédard, A. Adamo, K. C. Aroh, M. G. Russell, A. A. Bedermann, J. Terosian, B. Yue, K. F. Jensen, T. F. Jamison, *Science* **2018**, *361*, 1220.
[28] T. Bretschneider, C. Ozbal, M. Holstein, M. Winter, F. H. Buettner, S. Thamm, D. Bischodd, A. H. Luippold, *SLAS Technol.* **2019**, *24*, 386.
[29] Z. Jaman, A. Mufti, S. Sah, L. Avramova, D. H. Thompson, *Chem. Eur. J.* **2018**, *24*, 9546.
[30] M. Wleklinski, B. P. Loren, C. R. Ferreira, Z. Jaman, L. Avramova, T. J. P. Sobreira, D. H. Thompson, R. G. Cooks, *Chem. Sci.* **2018**, *9*, 1647.
[31] J. W. Sawicki, A. R. Bogdan, P. A. Searle, N. Talaty, S. W. Djuric, *React. Chem. Eng.* **2019**, *4*, 1589.
[32] P. W. Fedick, K. Iyer, Z. Wei, L. Ayramova, G. O. Capek, R. G. Cooks, *J. Am. Soc. Mass Spectrom.* **2019,** *30*, 2144.
[33] S. Shaabani, R. Xu, M. Ahmadianmoghaddam, L. Gao, M. Stahorsky, J. Olechno, R. Ellson, M. Kossenjans, V. Helan, A. Dömling, *Green Chem.* **2019**, *21*, 225.
[34] Y. Wang, S. Shaabani, M. Ahmadianmoghaddam, L. Gao, R. Xu, K. Kurpiewska, J. Kalinowska-Tluscik, J. Olechno, R. Ellson, M. Kossenjans, V. Helan, M. Groves, A. Dömling, *ACS Cent. Sci.* **2019**, *5*, 451.
[35] I. Sinclair, R. Stearns, S. Pringle, J. Wingfield, S. Datwani, E. Hall, L. Ghislain, L. Majlof, M. Bachman, *J. Lab. Autom.* **2016**, *21*, 19.
[36] I. Sinclair, M. Bachman, D. Addison, M. Rohman, D. C. Murray, G. Davies, E. Mouchet, M. E. Tonge, R. G. Stearns, L. Ghislain, S. S. Datwani, L. Majlof, E. Hall, G. R. Jones, E. Hoyes, J. Olechno, R. Ellson, P. E. Barran, S. D. Pringle, M. R. Morris, J. Wingfield, *Anal. Chem.* **2019**, *91*, 3790.
[37] K. J. DiRico, W. Hua, C. Liu, J. W. Tucker, A. S. Ratnayake, M. E. Flanagan, M. D. Troutman, M. C. Noe, *ACS Med. Chem. Lett.* **2020**, *11*, 1101.
[38] S. Sun, T. R. Slaney, R. T. Kennedy, *Anal. Chem.* **2012**, *84*, 5794.
[39] S. Sun, R. T. Kennedy, *Anal. Chem.* **2014**, *86*, 9309.
[40] X. W. Diefenbach, I. Farasat, E. D. Guetschow, C. J. Welch, R. T. Kennedy, S. Sun, *ACS Omega* **2018**, *3*, 1498.
[41] E. E. Kempa, C. A. Smith, X. Li, B. Bellina, K. Richardson, S. Pringle, J. L. Galman, N. J. Turner, P. E. Barran, *Anal. Chem.* **2020**, *92*, 12605.
[42] R. T. Kelly, J. S. Page, I. Marginean, K. Tang, R. D. Smith, *Angew. Chem., Int. Ed.* **2009**, *48*, 6832.
[43] D. J. Steyer, R. T. Kennedy, *Anal. Chem.* **2019**, *91*, 6645.
[44] T. Hatakeyama, D. L. Chen, R. F. Ismagilov, *J. Am. Chem. Soc.* **2006**, *128*, 2518.
[45] R. J. Beulig, R. Warias, J. J. Heiland, S. Ohla, K. Zeitler, D. A. Belder, *Lab Chip* **2017**, *17*, 1996.
[46] A. C. Sun, D. J. Steyer, A. R. Allen, E. M. Payne, R. T. Kennedy, C. R. J. Stephenson, *Nature Commun.* **2020**, *11*, 6202.
[47] C. K. Prier, D. A. Rankic, D. W. C. MacMillan, *Chem. Rev.* **2013**, *113*, 5322.
[48] N. A. Romero, D. A. Nicewicz, *Chem. Rev.* **2016**, *116*, 10075.
[49] R. C. McAtee, E. J. McClain, C. R. J. Stephenson, *Trends Chem.* **2019**, *1*, 111.
[50] J. J. Douglas, M. J. Sevrin, C. R. J. Stephenson, *Org. Process. Res. Dev.* **2016**, *20*, 11134.
[51] D. A. Nagib, D. W. C. MacMillan, *Nature* **2011**, *480*, 224.
[52] J. W. Beatty, J. J. Douglas, K. P. Cole, C. R. J. Stephenson, *Nat. Commun.* **2015**, *6*, 7919.
[53] J. W. Beatty, J. J. Douglas, R. Miller, R. C. McAtee, K. P. Cole, C. R. J. Stephenson, *Chem* **2016**, *1*, 456.
[54] R. C. McAtee, J. W. Beatty, C. C. McAtee, C. R. J. Stephenson, *Org. Lett.* **2018**, *20*, 3491.
[55] A. C. Sun, E. J. McClain, J. W. Beatty, C. R. J. Stephenson, *Org. Lett.* **2018**, *20*, 3487.
[56] M. Chabert, K. D. Dorfman, P. de Cremoux, J. Roeraade, J-L. Viovy, *Anal. Chem.* **2006**, *78*, 7722.
[57] Pfizer commercial compound library link: https://www.sigmaaldrich.com/life-science/cell-biology/bioactive-small-molecules/pfizer.html
[58] Development of an MS-MS assay can help to reduce, and possibly remove, background noise by increasing assay specificity towards the product of interest.
[59] We chose to use trifluoromethylated ethyltheophylline as the internal standard for our caffeine trifluoromethylation reaction, as it only varies in structure by a single methylene group from caffeine. This change is easily discernible by MS but should not significantly affect ionization.
[60] N. Thorne, M. Shen, W. A. Lea, A. Simeonov, S. Lovell, D. S. Auld, J. Inglese, *Chem. Biol.* **2012**, *19*, 1060.
[61] P. Ho, K. Yue, P. Pandey, L. Breault, F. Harbinski, A. J. McBride, B. Webb, J. Narahari, N. Karassina, K. V. Wood, A. Hill, D. S. Auld, *ACS Chem. Biol.* **2013**, *8*, 1009.

Entry for the Table of Contents

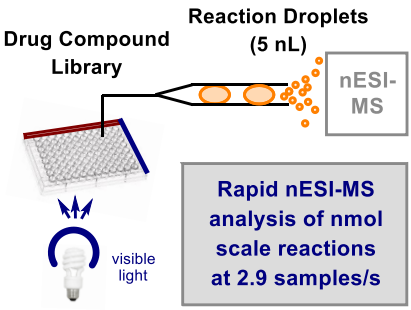

Insert text for Table of Contents here. ((maximum 450 characters including spaces; please provide a Table of Contents text that gives readers a short preview of the main theme of the research and results included in the paper to attract their attention into reading the paper in full. Define acronyms, including those in the picture! The Table of Contents text should be different from the abstract))

Segmented flow mass spectrometry was used to enable rapid screening of nanomole-scale photoredox reactions for drug discovery. Nanoelectrospray ionization mass spectrometry analysis was carried out at throughputs as high as 2.9 samples/s, allowing for the late-stage modification of complex drug scaffolds, as well as the subsequent structure-activity relationship (SAR) evaluation of prepared analogs.

Institute and/or researcher Twitter usernames: @AlexandraCSun, @crjsteph, @rtkenn, @MichiganChem